The Cryosphere Discuss., 5, 2629–2663, 2011
www.the-cryosphere-discuss.net/5/2629/2011/
doi:10.5194/tcd-5-2629-2011

The Cryosphere Discussions

Influence of surface heterogeneity on observed borehole temperatures at a mountain permafrost site in the Upper Engadine, Swiss Alps

S. Schneider, M. Hoelzle, and C. Hauck

Alpine Cryosphere and Geomorphology (ACAG), Department of Geosciences,
University of Fribourg, Fribourg, Switzerland

Received: 7 September 2011 – Accepted: 26 September 2011 – Published: 11 October 2011

Correspondence to: S. Schneider (sina.schneider@unifr.ch)

Published by Copernicus Publications on behalf of the European Geosciences Union.

Abstract

Compared to lowland (polar) regions, permafrost in high mountain areas occurs in a large variety of surface and subsurface material and texture. This work presents an eight-year (2002–2010) data set of borehole temperatures for five different (sub-) surface materials from a high alpine permafrost area, Murtel-Corvatsch, Switzerland. The influence of the material on the thermal regime was investigated by borehole temperature data, the TTOP-concept and the apparent thermal diffusivity (ATD). The results show that during the last eight years material specific temperature changes were more significant than for all boreholes consistent, climate-induced temperature trends. At coarse blocky, ice-rich sites no changes in active layer depth were observed, whereas the bedrock and the fine-grained sites appear to be highly sensitive to changes in the microclimate. The results confirm that the presence and growth of ice as well as a thermally driven air-circulation within the subsurface are the key factors for the occurence and preservation of alpine permafrost.

1 Introduction

In high moutain permafrost the thermal regime of the active layer strongly depends on site-specific factors like the albedo, the emissivity, the surface roughness, the grain size, the pore volume, the composition and type of material as well as climatic factors such as air temperature, incoming radiation and precipitation. As long as the surface of the bedrock is not covered by coarse or fine material and no snow is present, the thermal regime of the ground is directly coupled with the atmosphere (Williams and Smith, 1989) and the heat will mainly be transferred by conduction and advection of melt water (Wegmann et al., 1998, Gruber and Haeberli, 2007, Krautblatter and Hauck, 2007).

Permafrost degradation in bedrock is caused by frost weathering leading to a reduction of rock strength (Harris et al., 2009) as well as by advective processes by percolating meltwater. The degradation by advection can destabilize much greater volumes of rock than conduction within the same time (Gruber and Haeberli, 2007). Whereas air-ventilation within clefts can cause a lowering of the temperature of about 1.5 °C within strongly fractured near-vertical bedrock (Hasler et al., 2011). If the bedrock is covered by vegetation and soil the thermal responds of the active layer to surface temperatures will be damped. Moss and organic matter affect the hydrological properties, as they increase the water holding capacity of the soil (Walker et al., 2003).

If a buffer layer of coarse blocky material is present, density differences and processes like wind pumping lead to an exchange of air masses within the ground and enhance convective and advective air flows (Hanson and Hoelzle, 2004; Panz, 2006). Gruber and Hoelzle (2008) assume that a porosity of 40 % can reduce the thermal conductivity by about an order of magnitude compared to bedrock. One of the best known phenomenon within coarse blocky material is the cooling effect of reversible air circulation (the so called chimney-effect, described e.g. in Wakonigg, 1996; Sawada et al., 2003; Lambiel and Pieracci, 2008; Phillips et al., 2009 and Morard et al., 2010). In general, it is assumed that the chimney-effect can only develop under thin, non-insulating snow cover conditions. In contrast Delaloye and Lambiel (2005) showed that even in the presence of a thick snow cover, the ascent of relatively warm air within a blocky slope can force the aspiration of cold air through the snow cover into the blocks which reduces the temperature of the lower part of the slope. This thermally driven ventilation can lead to a cooling of the subsurface by several degrees.

A fine-grained buffer layer, with a high permeable texture supports the advective heat transport by infiltrating (snowmelt)-water. Hinkel and Outcalt (1994) suppose that the warming of fine-grained permafrost material in arctic lowlands by advective processes exceeds those by conduction by one or two orders of magnitude. The gravity infiltration of melt water may be enhanced by the transport of water and vapour in response to osmotic pressure gradients induced by relatively higher solute concentration at depth (Hinkel and Outcalt, 1994; Outcalt et al., 1990). Modelling the advective processes

Scherler et al. (2010) pointed out that the advective heat transport by percolating water is not negligible and seems to be a key factor to increase the temperature of the permafrost.

The snow cover as an additional seasonal buffer layer influences the thermal regime of the subsurface mainly as the thermal resistance of the snow cover increases with increasing snow depth. Haeberli (1973), Keller and Gubler (1993) and Hanson and Hoelzle (2004) observed in field studies and Luetschg et al. (2008) in modelled studies that effective thermal resistance exists at a snow depth of more than 0.6–0.8 m. By constant air temperature an increase of snow depth of 1 m (starting with a 0.2 m, non-insulating snow cover) can lead to an increase of the mean annual ground surface temperature (MAGST) by app. 2.7 °C (Luetschg et al., 2008). Gruber and Hoelzle (2008) pointed out that coarse blocky material can reduce the warming effect of the snow cover up to several degrees celcius due to the lower thermal conductivity at the near-surface of the blocky layer. Furthermore, the duration and date of the first significant snowfall in autumn, and the date of the disappearance of snow in spring, are important factors in terms of the thermal regime of the entire year. In model experiments Luetschg et al. (2008), showed that the longer the time span of a non-insultating snow cover, the colder the thermal regime of the entire year. Hereby, the cooling caused by delayed snowfall in autumn is within the same order of magnitude as the affect by delayed snow melt in spring (Ling and Zhang, 2003; Luetschg et al., 2008).

Since work on high altitude permafrost distribution started in the 1970's one of the challenging problems is the heterogeneity of mountain permafrost in terms of its microclimate, snow cover and subsurface material, which makes a direct comparison of different permafrost sites almost impossible. If this heterogeneity and its influence on the thermal regime of the permafrost is known, the accuracy of spatially distributed permafrost models based on topoclimatic factors could be verified. In this contribution, eight year time series of seasonal and inter-annual borehole temperature variability within a small (1 km^2) high mountain permafrost region with different surface and subsurface materials is presented. Local climatic factors (such as air temperature, wind speed and direction, relative humidity and incoming solar radiation) as well as the topographic situation (exposition, slope angle) are assumed to be the same for all boreholes. Hence observed differences in subsurface temperatures are mostly due to the different subsurface materials and their corresponding, material dependent, dominant processes. Since the aim of this work is to understand the different processes occuring in high mountain permafrost and to estimate the different sensitivities to changes in the microclimate, this work is focused on (1) the characterisation of the thermal regimes for different materials based on borehole temperature data from 2002–2010, (2) an analysis of the relationship between air temperature and subsurface temperature by using the extended TTOP concept and (3) an evaluation of the thermal response of the different subsurface materials by calculating the temperature transfer rate and the apparent thermal diffusivity.

2 Investigation site and data sets

The study area is situated in the Upper Engadin (Eastern Swiss Alps) at around 2700 m a.s.l. and is surrounded by a steep northwest facing rock wall (Fig. 1). Taking into account that the investigation of this area started in the 1970s (Barsch, 1977), it is now one of the best investigated permafrost areas in the Alps and part of the PERMOS network (Permafrost Monitoring Switzerland) (e.g. Haeberli et al., 1988; Vonder Muehll et al., 2001; Hoelzle et al., 2002; Hanson and Hoelzle, 2005 and Noetzli and Vonder Muehll, 2010). Within the area the Murtel rock glacier is one of the dominant periglacial features, but further rock glaciers and talus slopes are present to the west (Fig. 2). The borehole network consists of a 58 m deep borehole drilled on the rock glacier Murtel in 1987 (Haeberli et al., 1988), two boreholes drilled in 2002 on the nearby Chastelets rock glacier and three boreholes located in between (Hanson and Hoelzle, 2005). Though the climatic parameters can be assumed to be similar for all borehole sites, there is a strong variation of the subsurface material and ice content, in which the boreholes are drilled.

2.1 Air temperature measurements and snow height

A micrometeorological station located at the Murtel rock glacier measures air temperature, wind speed and direction, humidity, in- and outgoing longwave radiation, in- and outgoing shortwave radiation and the height of the snow cover since January 1997 (Mittaz et al., 2000). Data are recorded every 10 minutes and logged as means over 30 minute intervals. Since 2010 the data are recorded with an hourly interval. From 1988 until 2006, the mean annual air temperature (MAAT) was $-1.8\,^{\circ}\mathrm{C}$ and the avarage snow cover amount was 0.41 m (Hoelzle and Gruber, 2008). During the snow covered period, the ground surface temperature (GST) is estimated by an IR-thermometer which was added to the micrometeorological station in 2001 (Hoelzle and Gruber, 2008). The micrometeorological measurements at Murtel rock glacier are considered to be representative for the whole study area. However, to estimate the exact duration of the snow cover at each borehole site, GST measurements are used, as the treshold of the daily temperature amplitude of $0.4\,^{\circ}\mathrm{C}$ indicates whether snow is present ($\leq 0.4\,^{\circ}\mathrm{C}$) or not ($>0.4\,^{\circ}\mathrm{C}$).

2.2 Ground surface and subsurface temperature measurements

A temperature sensor which is placed at the surface next to each single borehole (Hanson and Hoelzle, 2005) will be used to obtain the GST for each borehole separately.

Subsurface temperatures are measured by temperature sensors which are placed within the six boreholes (Fig. 2). The borehole at the Murtel rock glacier (RMc) was drilled in coarse blocky material. Thermistors were placed down to 58 m depth, starting at 0.5 m and seperated by 1 m. The five boreholes which were drilled by Hanson and Hoelzle (2005) are each 6 m deep and equipped with 18 thermistors, which were placed every 10 cm within the uppermost meter, every 0.5 m from 1 to 5 m and at 6 m depth. Two of these boreholes were drilled in bedrock (one on bare bedrock, Bb, the other one is covered by 19 cm of soil and vegetation, Bv), one is situated on a coarse blocky talus slope (TSc), one was drilled in the fine-grained material of the Chastelets rock glacier close to its front (RCf) and the last one is located in the coarse blocky part of the Chastelets rock glacier (RCc) (Fig. 2).

3 Data processing

As a means to analyse the relative influence of different subsurface materials on the thermal regime, the relationship between air temperature and subsurface permafrost temperature can be estimated by using the extended TTOP-concept (Smith and Riseborough, 1996; Herz et al., 2003; Hoelzle and Gruber, 2008). The TTOP-concept was developed to explain the climate-permafrost relationship and describes the offset between the mean annual air temperature (MAAT) and the temperature at the top of the permafrost (TTOP) (Smith and Riseborough, 1996). To take into account the surface heterogeneity in mountain areas, the MAGST was added. The total offset between the air temperature and the temperature of the permafrost is expressed by an offset between MAAT and MAGST and an offset between MAGST and TTOP. Hoelzle and Gruber (2008) recommend to include a third temperature value, the mean annual surface temperature (MAST), which is the thermal infrared radiating temperature of the ground surface, measured by an IR thermometer. Therefore, the surface offset has to be partitioned into the offset between MAAT and MAST, and another between MAST and MAGST. This concept is particularly important for mountain permafrost environments, because the duration and the height of snow cover as well as its influence on the surface temperature can be taken into account.

Data processing is done individually for the four season: spring, summer, autumn and winter. As the seasonally varying micro-climatic parameters such as snow cover and infiltrating melt water can be site specific, it is important to adapt the seasons separately for each site, according to the dominant processes and not solely with respect to a fixed date. Spring is defined by the impact of the melt water leading to the zero curtain (i.e. maintaining temperatures near 0 °C for a considerable length of time due to the release of latent heat). Summer time is defined as the time between the end of the

TCD
5, 2629–2663, 2011
Influence of surface heterogeneity on observed borehole temperatures
S. Schneider et al.

spring zero curtain and the first time in autumn when the surface temperature drops below 0 °C. The autumn is characterized by temperatures below 0 °C but without the existence of an insulating snow cover. Whereas the winter season is characterized by a snow cover, which is thick enough to decouple the air temperature from the ground surface temperature. The thresholds used to determine the seasons in this study are shown in Table 1.

To estimate the thermal response of the different subsurface materials, the apparent thermal diffusivity and the temperature transfer rate was calculated for all sites for the period between 2003–2010. The thermal diffusivity describes the degree of how fast a material can change its temperature. It is expressed by the ratio of thermal conductivity to heat capacity. Its variations can be interpreted in terms of phase changes in the subsurface. In unfrozen material, increasing water content leads to an increase of the thermal diffusivity, which is due to a more rapid increase of conductivity than of heat capacity (Williams and Smith, 1989). Pogliotti et al. (2008) pointed out that the key factor of the ATD is the water content. In frozen materials, especially within the temperature range from 0 to −3 °C, the diffusivity is highly temperature dependent and is dominated by the heat capacity term (Williams and Smith, 1989). Note that estimating the thermal diffusivity by borehole temperature data include the effect of non-conductive heat transfer including water vapour transport and release of latent heat (apparent thermal diffusivity). Assuming that the temperature pattern can be described by an elementary sinusoidal function, the ATD was calculated by the yearly temperature amplitude according to Williams and Smith (1989):

$$k = \frac{\omega \left(z_1 - z_2\right)^2}{2\left[\ln\left(\frac{A_1}{A_2}\right)\right]^2} \tag{1}$$

where k is the thermal diffusivity [$m^2\,s^{-1}$], ω the signal frequency [$s^{-1}\,yr^{-1}$], z = depth [m], and A_1 and A_2 are the temperature amplitudes [K] at the depths z_1 and z_2 [m].

TCD
5, 2629–2663, 2011

The temperature transfer rate (T_R) describes the temperature change within the active layer with time.

$$T_R = \frac{\left(\frac{\Delta T}{\Delta t}\right)}{(z_1 - z_2)} \tag{2}$$

with:

$$\Delta T = T_{\mathrm{Max1}} - T_{\mathrm{Max2}} \tag{3}$$

$$\Delta t = t_{T_{\mathrm{Max1}}} - t_{T_{\mathrm{Max2}}} \tag{4}$$

The temperature change with depth (ΔT [K]) is expressed as the temperature difference between the annual maximum temperature at depth 1 (T_{Max1}) and depth 2 (T_{Max2}) whereas $z_1 = 0.5$ m and $z_2 =$ depth of TTOP [m], Δt is the time interval [d] between $t_{T_{\mathrm{Max1}}}$ and $t_{T_{\mathrm{Max2}}}$.

4 Results

4.1 Eight years of active layer observation at the Murtel Corvatsch Area

The development of the subsurface temperature is shown for all six boreholes from 2002 until 2010 (Fig. 3). At all sites minimum winter temperatures were observed in 2004/2005 and 2005/2006 due to a low, non insulating snow cover. In summer the bedrock sites (Fig. 3a and b) are unfrozen down to 6 m depth. During the last two years, the Bb site (Fig. 3a) did not freeze at all below 5 m depth. Seasonal temperature fluctuations at the surface are within a range of −13 to 25 °C. In Fig. 3b an anomaly of strongly increasing temperatures at approximately 5 m depth is visible. Concerning the ground cooling in autumn, both sites seem to have a threshold (Bb at 0.5 and 1.5 m depth, respectively Bv at 1 m) at which the freezing process is decelerated.

Figure 3c shows the observed temperature evolution of the borehole drilled in the talus slope (TSc). The borehole is only 25 m away from the bedrock sites but it shows a completely different temperature regime: (1) permanently frozen conditions below 5 m, (2) a smaller seasonal temperature variation (3) a variable active layer. The depth of the active layer of the rock glacier sites never exceeds 3 m (RCc, Fig. 3e) or 3.5 m (RMc, Fig. 3f). During winter these sites experience the lowest temperatures within the permafrost body compared to the other sites. Seasonal temperature fluctuations at the surface are within a range of −15 until 28 °C and therefore similar to those of the bedrock sites.

In summer 2009 the thermistor chain of the RCc borehole was cut at about 4m depth due to the movement of the rock glacier. Hence it can be assumed that its shear horizon is at 4 m depth, 1.5 m below the top of permafrost. Finally, Fig. 3d presents the temperature of the borehole, which is located at the front of the Chastelets rock glacier (RCf) and which is drilled in fine-grained material. Since 2009, no more permafrost was observed within 6 m of the borehole. The thermal regime shows a similar pattern as that at the TSc site (Fig. 3c), but summer temperatures at the surface are lower and the active layer is much deeper than at the TSc.

Regarding the annual change of active layer depth (Fig. 4) during the last eight years, a range of 3.5–5.5 m for TSc and 4–6 m for RCf is remarkable. The year 2005 shows the shallowest active layer depth whereas during the years 2003 and 2009 the depth was up to 6 m at the fine-grained and 5.5 m at the talus slope site. In general, two patterns can be distinguished: (a) the RCf and the TSc site, which show a high inter-annual variability and (b) the coarse blocky rock glacier sites (RCc and RMc), at which the active layer depth remains constant each year.

4.2 Influence of the subsurface material on the ground thermal regime

Though all sites are influenced by the same meteorological input values, the temperatures at the surface und the subsurface vary according to the site-specific material.

Mean winter air temperature (defined according to Table 1) is −6.5 °C and mean summer air temperature is 5.2 °C, whereas mean ground surface temperatures differ from −4.9 (RMc) to −2.2 °C (TSc) in winter and from 5.7 (TSc) to 9.2 °C (Bv) in summer. Comparing all sites, it becomes apparent that the bedrock sites (Fig. 5a and b) experience an almost linear temperature decrease with depth in summer (respectively increase in winter). As already noticed in Fig. 3b, the anomaly at 5–6 m depth at the Bv site leads to increasing summer and decreasing winter temperatures at the bottom of this borehole. The TSc site (Fig. 5c) shows a large temperature gradient within the first meter and a smaller gradient from 1–6 m depth. Below 3.5 m, the eight year mean temperatures are around 0 °C throughout the year. All rock glacier sites (Fig. 5d–f) show a splitted temperature profile, including an upper part (active layer) with a high temperature gradient and the permanently frozen part below with almost homogeneous temperatures. At the RCc and RMc sites (Fig. 5e and f) the temperature within the permafrost body varies between −2.3 (winter mean) and −0.5 °C (summer mean). The temperature of the rock glacier front (RCf Fig. 5d) remains always around 0 °C, indicating that phase change processes take place.

To analyse the seasonal influence of the surface and subsurface material, cumulative temperatures were calculated and are shown in Fig. 6. Starting at the first of October of each year the daily mean temperatures were summed up for one year and presented as a four-year mean. Cumulative temperatures give evidence about the yearly balance of a thermal regime. In permafrost, the cumulative mean temperatures should be negative over the course of one year, and for positive cumulative mean temperatures, seasonal frost can be assumed. Figure 6a presents cumulative mean temperatures of the surface of different materials and of the air temperature at 2 m height. The highest cumulative temperatures after one year are found for the bedrock sites (Bb and Bv). Even though the cumulative mean air temperature is clearly negative, all sites apart from RMc, show positive cumulated temperatures at the surface (0 m). The largest difference (1626 K) is between the air temperature and the temperature of Bv. At all sites the cumulative temperatures within the thaw layer increase much faster during summer than the temperatures are decreasing in winter (Fig. 6b). Hence, the thermal permafrost regime remains stable, if the higher amount of freezing degree days compensates the faster increase of summer temperatures. This is only observed at the rock glacier sites, which show a clear negative temperature trend at a depth of 2.5 m. The TSc and the RCf sites are close to 0 K, which is mainly due to a much smaller temperature decrease in winter. Comparing the two boreholes of the Chastelets rock glacier (RCc and RCf), cumulative temperatures for RCf are 792 K higher than for RCc. Although the temperature increase during summer is the same, RCf experiences less cooling during winter.

Presenting cumulative temperatures at 5 m depth in Fig. 6c, permafrost and seasonal frost regimes can be differentiated. The only sites with a stable permafrost regime are the coarse blocky rock glaciers (RMc and RCc). The TSc and the RCf site have an intermediate regime close to 0 K.

By comparing the bare and the vegetated bedrock sites (Fig. 7a and b), the Bv site shows 50 K higher cumulated mean temperatures, but a smaller amount of freezing degree days (126 K) and a smaller amount of thawing degree days (77 K) than Bb. Although the borehole is only covered by 19 cm of soil and vegetation, this effect has an impact on the thermal regime until >1 m depth (Fig. 7c)

The differences of the yearly freezing and thawing periods are listed in detail for the uppermost sensors at each borehole in Table 2. The rock glacier sites (RCc and RMc) have a mean of 250 freezing degree days each year and therefore much more than the seasonal frost sites (Bb and Bv). In the years 2005 and 2006 all sites experienced the strongest cooling (i.e. the highest cumulative freezing temperature gradient (CFTG)). During the warm summer in 2003 the cumulative thawing temperature gradient (CTTG) was only slightly increased, whereas the CFTG was at all sites one of the lowest during the last eight years. In general the cumulative freezing temperature gradient (CFTG) is lower at all sites and in all years than the cumulative thawing temperature gradient (CTTG), except in the year 2006 where at the rock glacier and the talus slope places the CFTG exceeds the CTTG. At each site the annual change of the CFTG is higher

TCD
5, 2629–2663, 2011

(standard deviation between 0.91 and 2.72) than the annual change of the CTTG with a standard deviation between 0.38 and 1.27.

4.3 Apparent thermal diffusivity (ATD)

Figure 8 presents the calculated ATD for different sites and depths. Only values below 1m depth will be discussed, because the temperature amplitude close to the surface is influenced by energy balance parameters rather than by thermal properties of the subsurface. ATD values found within the active layer of the Chastelets rock glacier (1–3 m) are about $1.8 \times 10^{-6}\,m^2\,s^{-1}$ and therefore higher than within the ice-filled permafrost layer underneath (0.7×10^{-6}–$1.2 \times 10^{-6}\,m^2\,s^{-1}$). These values agree well with the ones published by Williams and Smith (1989) where pure ice is given by a value of $1.16 \times 10^{-6}\,m^2\,s^{-1}$ at 0 °C. The permafrost layer of RMc (3–5 m) shows values between 0.48×10^{-6}–$0.52 \times 10^{-6}\,m^2\,s^{-1}$, which are therefore slightly lower and have a smaller range (Fig. 8). According to Hooke (1998) at a temperature of −0.5 °C variations of the ATD are mainly caused by changes in thermal conductivity, which is slightly decreasing with increasing temperatures. On the other hand, the heat capacity is increasing because of a continuously rising unfrozen water content within the ice. However, real conditions influencing the ATD of rock glaciers are even more complicated because heat capacity is also depending on the concentration of impurities in the ice, and the thermal conductivity is influenced by the ratio of ice/rock. The ATD of the bedrock sites increases with depth to values up to $0.7 \times 10^{-6}\,m^2\,s^{-1}$, which is slightly lower than the ones of Robert (1998), who found $1.7 \times 10^{-6}\,m^2\,s^{-1}$ as value for granitic rock at a MAST of around 7.2 °C. The talus slope and the fine grained site at the Chastelets rock glacier show values of $1.0 \times 10^{-6}\,m^2\,s^{-1}$ within 1–3 m and $0.65 \times 10^{-6}\,m^2\,s^{-1}$ (TSc) or $1.2 \times 10^{-6}\,m^2\,s^{-1}$ (RCf) within 3–5 m depth.

Figure 9 presents the calculated temperature transfer rate for different sites. As expected the rock glacier sites (RCc and RMc) have the fastest temperature transfer, followed by the talus slope and by the bedrock and fine-grained sites. Consequently the ice within the rock glaciers enhances the temperature gradient and therefore the temperature transfer rate of a factor of four (up to 5.6 $K m^{-1} d^{-1}$) compared to the ice-free sites.

5 Discussion

The investigated sites in the Murtel-Corvatsch area show no consistent subsurface temperature trends since 2002 within the observed range of depth. Rather, the thermal regime is mainly influenced by the composition of the subsurface material. The two bedrock sites (Bb and Bv) showed only seasonal frost within the investigated range of depth and increased temperatures were observed in 2003, 2008 and 2009. At the Bb site (below 5 m depth) no freezing was observed during the last two years (Fig. 3a). This might be caused by additional heating through the SW-exposition of the bedrock outcrop nearby (Fig. 1). The coarse blocky, ice-rich rock glacier sites (RCc and RMc) showed no significant changes in the thermal regime during the entire observation period (Figs. 3 and 4). Their temperature profile is split into a high temperature gradient (from 0.5 m depth to TTOP) and almost isothermal temperature conditions of the ice within the permafrost. The fine-grained site at the frontal part of the Chastelets rock glacier (RCf) became ice free in 2008 or 2009 (see Fig. 3d). All sites apart from RMc, showed positive cumulated temperatures at the surface, even though the cumulative mean air temperature is clearly negative. This is caused by the isolating effect of the snow cover in winter. At all sites the cooling during autumn/winter and the duration of the zero curtain in spring had a stronger influence on the interannual variability of the thermal regime than temperature increase during summer (Table 2 and Fig. 6). In the following the dominant processes and material characteristics are discussed for each site:

- *Bedrock:* At the bedrock sites, thermal conduction was the dominant process as could be seen from the almost linear temperature decrease with depth (Fig. 5), the high cumulative thawing temperature gradient (CTTG) (9.4 °C day^{-1}) and the calculated ATD of about $0.7 \times 10^{-6}\,m^2\,s^{-1}$. In Bv (Fig. 3b) an anomaly of strongly increasing temperatures at approximately 5 m depth were visible. This might have been caused by a heterogeneity (e.g. a crack in the bedrock), allowing convective heat transfer. Comparing the vegetated with the bare bedrock site revealed that the Bv site shows 50 K higher cumulated mean temperatures, but a smaller amount of freezing degree days (126 K) and a smaller amount of thawing degree days (77 K) than Bb. Consequenly, the bare bedrock site experiences a higher incoming shortwave radiation during the day and a higher outgoing longwave radiation during the night. These two radiation fluxes seem to counter act in a quite homogenous way, whereas the Bv site dampens the daily temperature fluctuation due to a higher heat storage capacity of the soil (Walker et al., 2003), leading to a more balanced but slightly warmer regime. Consequently, the impact of the heat storage capacity on the annual thermal regime is more important than a slightly higher incoming solar radiation. This effect had an impact on the thermal regime until more than 1 m depth (Fig. 7c).

– *Rock glacier (coarse blocky):* The active layer depth of the two rock glaciers did not change during the last eight years (Fig. 4) and the temperature gradient within the active layer is the largest in comparison with the other sites (Fig. 5). The thermal regime seems to be strongly influenced by the comparatively high ice content causing only little variation of the active layer depth in spite of changing climate parameters. ATD values found within the active layer of the Chastelets rock glacier (1–3 m) are about $1.8 \times 10^{-6}\,m^2\,s^{-1}$ and therefore higher than at the ice-filled permafrost layer underneath ($0.9 \times 10^{-6}\,m^2\,s^{-1}$), caused by a higher amount of air filled pore spaces. The ATD values of the active layer and the high temperature transport rate of $5.6\,K\,m^{-1}\,d^{-1}$ (Fig. 9) confirm a high thermal response of the active layer. However, the thermal regime of the ice-rich rockglacier sites has been stable over the course of the last eight years.

TCD
5, 2629–2663, 2011

- *Rock glacier (fine-grained):* The variable active layer depth within the observed period of time and the temperature of the ice close to 0 °C illustrate the high sensitivity of this site. In the year 2008/2009 the remaining ice in the front of the rock glacier melted out completely (Fig. 3d), probably due to 3-D influenced topography of the rockglacier front (Fig. 1). The high temperature gradient within the active layer (Fig. 5d) was probably caused by the cold temperatures of the adjacent ice of the rock glacier. The duration of the zero curtain seems to be very important for this site, as shortening the thawing period of time. Still, some questions regarding the different processes at this site remain open and more field measurements would be necessary. Especially, detailed measurements of infiltration processes caused by (melt-) water, the impact of snow, and the amount and size of pore spaces have to be taken into account.

- *Talus slope:* A longer lasting snow cover and a reduced amount of incoming shortwave radiation, due to the slightly more shaded position between the blocks, caused a much longer frozen season (Figs. 3c and 5c) and lower cumulated temperatures at the surface (4.9 K) (Table 2) than at the bedrock sites beneath. Relative low MAAT during the year 2005 and 2006 (Fig. 3, Vonder Muehll et al., 2007) caused a shallow active layer depth whereas during the year 2003 and 2009 the active layer depth increased about 2m due to a relative high MAAT (Fig. 3, Noetzli and Vonder Muehll, 2010). The varying zero curtain in spring (Table 2) indicated highly variable from year to year production of ice during autumn/winter. However, the high interannual variability of active layer depth (Fig. 4) and the variable ATD values, lead to the assumption that this site had a yearly changing amount of ice/water as well as air-filled pore spaces but contained only very little ice during summer. Convective cooling by air flow between the blocks seemed to be efficient below 1m depth and caused low temperatures throughout the year. It can assumed that this site is mainly influenced by non-conductive processes as discussed in Delaloye and Lambiel (2005) and Lambiel and Pieracci (2008). Within the first meter a temperature transfer rate of about 2.1 $K\,m^{-1}\,d^{-1}$ was observed

(Fig. 9). As explained by Hanson and Hoelzle (2005), the first meter, of this borehole was drilled in a block of approximately 1m depth, leading to the assumption that the uppermost part of the borehole is dominated by conductive processes. Hence, the occurence of permafrost at this site, is due to the very efficient cooling by convective processes and the seasonal creation of ice.

6 Conclusions

Eight year borehole temperature data from a high alpine permafrost environment including different subsurface materials were presented. Assuming that the microclimate, the exposition and slope angle are almost the same for all sites, no uniform subsurface temperature changes were observed. The ground temperatures and the thermal regimes depend strongly on the subsurface material and its site specific processes as follows:

- At all sites the interannual variability of the cooling during autumn/winter and the duration of the zero curtain in spring have a stronger influence on the annual thermal regime than temperatures during summer, which showed less variability.
- At the investigated Murtel-Corvatsch area, temperature anomalies like the year 2003 (Vonder Muehll et al., 2007), are not due to a stronger temperature increase during summer rather than to the low cooling during the winter before.
- Within fine-grained material with a thermal regime close to 0 °C, the duration of the zero curtain seems to be a key factor for the thermal regime. During winter, fine-grained material experiences much less cooling than coarse blocky material.
- The height of the snowpack has an influence on all sites. A thin, snow pack without thermal resistance (i.e. during winter 2004/2005 and 2005/2006) forces a cooling of the ground irrespective of the subsurface material. Modelled results of Luetschg et al. (2008) could therefore be confirmed.

TCD
5, 2629–2663, 2011

- Ice-rich material enhances the temperature transport rate significantly due to a high temperature gradient. However, as long as the temperature of the ice is $< -1\,^{\circ}$C, the energy is used for phase change processes at the TTOP and no changes in active layer depth will occur.
- Within coarse blocky material, the air ventilation and the seasonal production of ice are the main factors for permafrost occurence in high alpine regions. While temperatures within the talus slope are close to $0\,^{\circ}$C and a stable permafrost regime is observed, the thermal regime of the fine-grained site (where convective and advective airflow can be neglected) thawed in 2008/2009.
- A vegetation and soil layer dampens the annual temperature amplitude deeper than 1 m. However, in total, the annual mean ground temperatures are higher as a result of the higher heat storage capacity of the soil.

Especially fine-grained material and material with small amounts of ice at a temperature of $0\,^{\circ}$C are highly sensitive to changes in the microclimate but these are not yet sufficiently investigated at these sites. The understanding of the processes during the phase change and its effect on different physical parameters is still challenging. Within fine-grained material numerous complex processes like the infiltration of melt (-water), refreezing water during summer and air-circulation depending on the pore spaces are involved, which should be further investigated by combined modelling and field studies.

Acknowledgements. The authors wish to express their thanks to the PERMOS network which provided the Murtèl borehole data, the Corvatsch AG for their friendly logistic support, Hansueli Gubler for its technical help and advice, the SPCC-project (Sensitivity of Mountain Permafrost to Climate Change) and Reynald Delaloye for their helpful discussions and lastly all who have contributed by the data aquisition in the field. This investigation was founded by the University of Fribourg, Switzerland.

References

Barsch, D.: Ein Permafrostprofil aus Graubuenden, Schweizer Alpen, Z. Geomorphol., 21, 79–86, 1977. 2633

Delaloye, R. and Lambiel, C.: Evidence of winter ascending air circulation throughout talus slopes and rock glaciers situated in the lower belt of alpine discontinous permafrost (Swiss Alps), Norw. J. Geogr., 59, 194–203, 2005. 2631, 2644

Gruber, S. and Haeberli, W.: Permafrost in steep bedrock slopes and its temperature-related destabilization following climate change, J. Geophys. Res., 112, F02S18, doi:10.1029/2006JF000547, 2007. 2630, 2631

Gruber, S. and Hoelzle, M.: The cooling effect of coarse blocks revisited, in: Proceedings of the 9th International Conference on Permafrost, edited by: Kane, D. L. and Hinkel, K. M., vol. 1, 557–561, 2008. 2631, 2632

Haeberli, W.: Die Basistemperatur der winterlichen Schneedecke als moeglicher Indikator fuer die Verbreitung von Permafrost in den Alpen, Z. Gletscherkd. Glazialgeol., 9, 221–227, 1973. 2632

Haeberli, W., Huder, J., Keusen, H., Pika, J., and Rothlisberger, H.: Core drilling through rock glacier-permafrost, in: 5th International Conference on Permafrost, Tapir Publishers, 937–942, 1988. 2633

Hanson, S. and Hoelzle, M.: The thermal regime of the active layer at the Murtèl rock glacier based on data from 2002, Permafrost Periglac., 15, 273–282, 2004. 2631, 2632

Hanson, S. and Hoelzle, M.: Installation of a shallow borehole network and monitoring of the ground thermal regime of a high alpine discontinuous permafrost environment, Norsk Geografisk Tidsskrift – Norw. J. Geogr., 59, 84–93, 2005. 2633, 2634, 2645

Harris, C., Arenson, L., Christiansen, H., Etzelmueller, B., Frauenfelder, R., Gruber, S., Haeberli, W., Hauck, C., Hoelzle, M., Humlum, O., Isaksen, I., Kaeaeb, A., Kern-Luetschg, M., Lehning, L., Matsuoka, N., Murton, Noetzli, J., Phillips, M., Ross, N., Seppaelae, M., Springman, S., and Vonder Muehll, D.: Permafrost and climate in Europe: Monitoring and modelling thermal, geomorphological and geotechnical responses, Earth-Sci. Rev., 92, 117–171, 2009. 2630

Hasler, A., Gruber, S., and Haeberli, W.: Temperature variability and thermal offset in steep alpine rock and ice faces, The Cryosphere Discuss., 5, 721–753, doi:10.5194/tcd-5-721-2011, 2011. 2631

Herz, T., King, L., and Gubler, H.: Microclimate within coarse debris of talus slopes in the alpine periglacial belt and its effect on permafrost, in: 8th International Conference on Permafrost, 383–387, 2003. 2635

Hinkel, K. and Outcalt, S.: Identification of heat-transfer process during soil cooling, freezing and thaw in central alaska, Permafrost Periglac., 5, 217–235, 1994. 2631

Hoelzle, M. and Gruber, S.: Borehole and Ground Surface Temperatures and their relationship to meteorological conditions in the Swiss Alps, in: Proceedings of the 9th International Conference on Permafrost, edited by: Kane, D. L. and Hinkel, K. M., vol. 1, 723–728, 2008. 2634, 2635

Hoelzle, M., Vonder Mühll, D., and Haeberli, W.: Thirty years of permafrost research in the Corvatsch-Furtschellas area, Eastern Swiss Alps: a review, Norsk Geografisk Tidsskrift – Norw. J. Geogr., 56, 137–145, 2002. 2633

Hooke, R.: Principles of glacier mechanics, Simon and Schuster/A Viacom Company, 1998. 2641

Keller, F. and Gubler, H.: Interaction between snow cover and high mountain permafrost, Murtèl-Corvatsch, Swiss Alps, in: Proceedings of the 6th International Conference on Permafrost, 5–9 July 1993, edited by: Cheng, G., South China University of Technology Press, Guangzhou, 332–337, 1993. 2632

Krautblatter, M. and Hauck, C.: Electrical resistivity tomography monitoring of permafrost in solid rock walls, J. Geophys. Res., 112, F02S20, doi:10.1029/2006JF000546, 2007. 2630

Lambiel, C. and Pieracci, K.: Permafrost distribution in talus slopes located within the alpine periglacial belt, Swiss Alps, Permafrost Periglac., 19, 293–304, 2008. 2631, 2644

Ling, F. and Zhang, T.: Impact of the timing and duration of seasonal snow cover on the active layer and permafrost in the Alaskan Arctic, Permafrost Periglac., 14, 141–150, 2003. 2632

Luetschg, M., Lehning, M., and Haeberli, W.: A sensitivity study of influencing warm/thin permafrost in the Swiss Alps, J. Glaciol., 54, 696–704, 2008. 2632, 2645

Mittaz, C., Hoelzle, M., and Haeberli, W.: First results and interpretation of energy-flux measurements of Alpine permafrost, Ann. Glaciol., 31, 275–280, 2000. 2634

Morard, S., Delaloye, R., and Lambiel, C.: Pluriannual thermal behavior of low elevation cold talus slopes in western Switzerland, Geogr. Helvetica, 2, 124–134, 2010. 2631

Noetzli, J. and Vonder Muehll, D.: Permafrost in Switzerland 2006/2007 and 2007/2008, Glaciological Report (Permafrost), vol. 8/9, Permafrost Monitoring Switzerland (PERMOS), Cryospheric Commission, 2010. 2633, 2644

Outcalt, S., Nelson, F., and Hinkel, K.: The zero-curtain effect: heat and mass transfer across an isothermal region in freezing soil, Water Resour. Res., 26, 1509–1516, 1990. 2631
Panz, M.: Analyse von Austauschprozessen in der Auftauschicht des Blockgletschers Murtèl-Corvatsch, Oberengadin, Master's thesis, Ruhr Universität, unpublished, 2006. 2631
Phillips, M., Zenklysen Mutter, E., Kern-Luetschg, M., and Lehning, M.: Rapid degradation of ground ice in a ventilated talus slope: Flueela Pass, Swiss Alps, Permafrost Periglac., 20, 1–14, 2009. 2631
Pogliotti, P., Cremonese, E., Morra di Cella, U., Gruber, S., and Giardino, M.: Thermal diffusivity variability in alpine permafrost rock walls, in: Proceedings of the 9th International Conference on Permafrost, edited by: Kane, D. L. and Hinkel, K. M., vol. 2, 1427–1432, 2008. 2636
Robert, S. A.: Near-surface thermal profiles in alpine bedrock: implications for the frost weathering of rock, Arct. Alpine Res., 30, 362–372, 1998. 2641
Sawada, Y., Ishikawa, M., and Yugo, O.: Thermal regime of sporadic permafrost in a block slope on Mt. Nishi-Nupukaushinupuri, Hokkaido Island, Northern Japan, Geomorphology, 53, 121–130, 2003. 2631
Scherler, M., Hauck, C., Hoelzle, M., Staehli, M., and Voelksch, I.: Melt-water infiltration into the frozen active layer at an alpine permafrost site, Permafrost Periglac., 21, 325–334, 2010. 2632
Smith, M. W. and Riseborough, D. W.: Permafrost monitoring and detection of climate change, Permafrost Periglac., 7, 301–309, 1996. 2635
Vonder Muehll, D., Arenson, L., and Springman, S.: Two new boreholes through the Murtèl-Corvatsch rock glacier, Upper Engadin, Switzerland, in: 1st European Permafrost Conference, edited by: Rea, B., 48–49, 2001. 2633
Vonder Muehll, D., Noetzli, J., Roer, I., Makowski, K., and Delaloye, R.: Permafrost in Switzerland 2002/2003 and 2003/2004, Glaciological Report (Permafrost), vol. 4/5, Permafrost Monitoring Switzerland (PERMOS), Cryospheric Commission, 2007. 2644, 2645
Wakonigg, H.: Unterkuehlte Schutthalden. Beitrge zur Permafrostforschung in Oesterreich, in: Arbeiten aus dem Institut fuer Geographie, vol. 33, Karl-Franzens-University, 209–223, 1996. 2631
Walker, D. A., Jia, G., Epstein, H., Raynolds, M., Chapin III, F., Copass, C., Hinzman, L., Knudson, J., Maier, H., Michaelson, G., Nelson, F., Ping, C., Romanovsky, V., and Shiklomanov, N.: Vegetation-soil-thaw-depth relationships along a Low-Artic bioclimate gradient, Alaska: Synthesis of information from the ATLAS studies, Permafrost Periglac., 14, 103–123, 2003.

TCD
5, 2629–2663, 2011

2631, 2643
Wegmann, M., Gudmundsson, G. H., and Haeberli, W.: Permafrost changes in rock walls and the retreat of alpine glaciers: a thermal modelling approach, Permafrost Periglac., 9, 23–33, 1998. 2630
Williams, P. J. and Smith, M. W.: The frozen earth – fundamentals of geocryology, Cambridge University Press, 1989. 2630, 2636, 2641

TCD
5, 2629–2663, 2011

Influence of surface heterogeneity on observed borehole temperatures

S. Schneider et al.

Table 1. Thresholds to differentiate the four seasons individually at each borehole.

Threshold	Spring	Summer	Autumn	Winter
Daily mean air temperature	≥0 °C	≥0 °C	<0 °C	<0 °C
Daily amplitude of GST	=0 °C	>0.4 °C	>0.4 °C	≤0.4 °C
Snow height (d)	–	–	$0 < d \leq 30$ cm	>30 cm

TCD
5, 2629–2663, 2011

Table 2. Comparison of freezing and thawing indicators for the last eight years and for different sites for 1.5 m depth. Freezing indicators are the cumulated freezing temperature gradient (CFTG), the annual amount of freezing days and the duration of the spring zero curtain. Thawing indicators are expressed by the cumulated thawing temperature gradient (CTTG) and the annual amount of thawing days. Values are calculated for hydrological years (i.e. 2003 starts at the 1 October 2002).

		freezing indicators			thawing indicators	
site	year	duration of spring zero curtain [d]	cumulative freezing temperature gradient (CFTG) [°C d^{-1}]	amount of freezing days	cumulative thawing temperature gradient (CTTG) [°C d^{-1}]	amount of thawing days days
Bb	2003	2	−0.13	84	11.3	279
	2004	–	–	–	–	–
	2005	5	−5.37	163	8.41	197
	2006	1	−4.59	186	8.84	178
	2007	–	–	–	–	–
	2008	–	–	–	–	–
	2009	0	0	0	9.56	365
	2010	0	0	0	9.16	365
mean (stdev)		2 (±2)	−2.02 (±2.72)	61 (±88)	9.45 (±1.11)	277 (±89)
Bv	2003	4	−0.13	51	10.8	310
	2004	–	–	–	–	–
	2005	1	−3.09	187	8.4	177
	2006	1	−2.92	200	8.92	164
	2007	–	-	–	–	–
	2008	–	–	–	–	–
	2009	0	−0.03	79	9.87	286
	2010	1	−0.05	100	8.77	264

TCD
5, 2629–2663, 2011

Table 2. Continued.

site	year	freezing indicators			thawing indicators	
		duration of spring zero curtain [d]	cumulative freezing temperature gradient (CFTG) [°C d^{-1}]	amount of freezing days	cumulative thawing temperature gradient (CTTG) [°C d^{-1}]	amount of thawing days days
mean (stdev)		1 (±2)	−1.24 (±1.61)	128 (±53)	9.35 (±0.97)	240 (±66)
TSc	2003	10	−0.07	121	5.9	234
	2004	–	–	–	–	–
	2005	6	−3.02	206	3.29	153
	2006	5	−3.78	225	2.91	135
	2007	–	–	–	–	–
	2008	–	–	–	–	–
	2009	4	−0.07	142	4.92	219
	2010	8	−0.84	177	3.38	180
mean (stdev)		7 (±2)	−1.56 (±1.73)	187 (±42)	4.08 (±1.27)	184 (±42)
RMc	2003	–	–	–	–	–
	2004	21	−3.31	237	5.48	108
	2005	19	−4.79	209	4.86	137
	2006	26	−5.64	218	5.27	121
	2007	–	–	–	–	–
	2008	25	−4.33	226	5.65	115
	2009	–	–	–	–	–
	2010	17	−3.73	236	5.84	112
mean (stdev)		22 (±4)	−4.36 (±0.91)	254 (±10)	5.42 (±0.38)	119 (±11)
RCc	2003	44	−1.39	224	6.82	97
	2004	41	−2.55	229	4.44	96
	2005	21	−5.23	225	4.33	119
	2006	24	−6.11	217	4.15	124
	2007	29	−3.86	174	5.56	162
	2008	–	–	–	–	–
	2009	–	–	–	–	–
	2010	43	−3.4	236	3.95	86

TCD
5, 2629–2663, 2011

Table 2. Continued.

site	year	freezing indicators: duration of spring zero curtain [d]	freezing indicators: cumulative freezing temperature gradient (CFTG) [°C d^{-1}]	freezing indicators: amount of freezing days	thawing indicators: cumulative thawing temperature gradient (CTTG) [°C d^{-1}]	thawing indicators: amount of thawing days days
mean (stdev)		34 (±10)	−3.76 (±1.73)	251 (±28)	4.88 (±1.11)	114 (±28)
RCf	2003	40	−0.98	181	6.25	144
	2004	38	−1.77	152	5.94	176
	2005	33	−4.43	142	5.23	190
	2006	14	−3.49	157	6.36	194
	2007	39	−2.58	116	5.36	210
	2008	–	–	–	–	–
	2009	–	–	–	–	–
	2010	43	−0.32	32	6.78	290
mean (stdev)		35 (±11)	−2.26 (±1.55)	165 (±49)	5.99 (±0.60)	201 (±49)

TCD
5, 2629–2663, 2011

Influence of surface heterogeneity on observed borehole temperatures

S. Schneider et al.

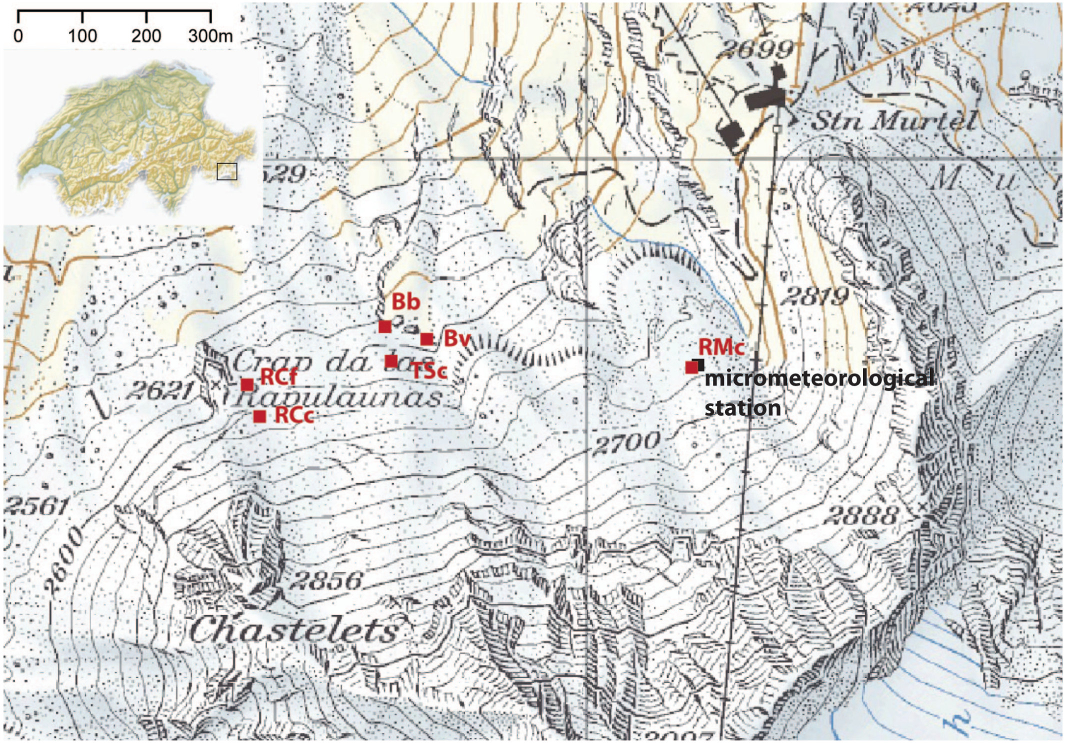

Fig. 1. Investigation area Murtel-Corvatsch, Eastern Swiss Alps. The 5 shallow boreholes are indicated by its material: Bb = bare bedrock, Bv = vegetated bedrock, TSc = talus slope (coarse blocky), RCf = rock glacier Chastelets (fine-grained), RCc = rock glacier Chastelets (coarse blocky) and RMc rock glacier Murtel (coarse blocky).

TCD
5, 2629–2663, 2011

Influence of surface heterogeneity on observed borehole temperatures

S. Schneider et al.

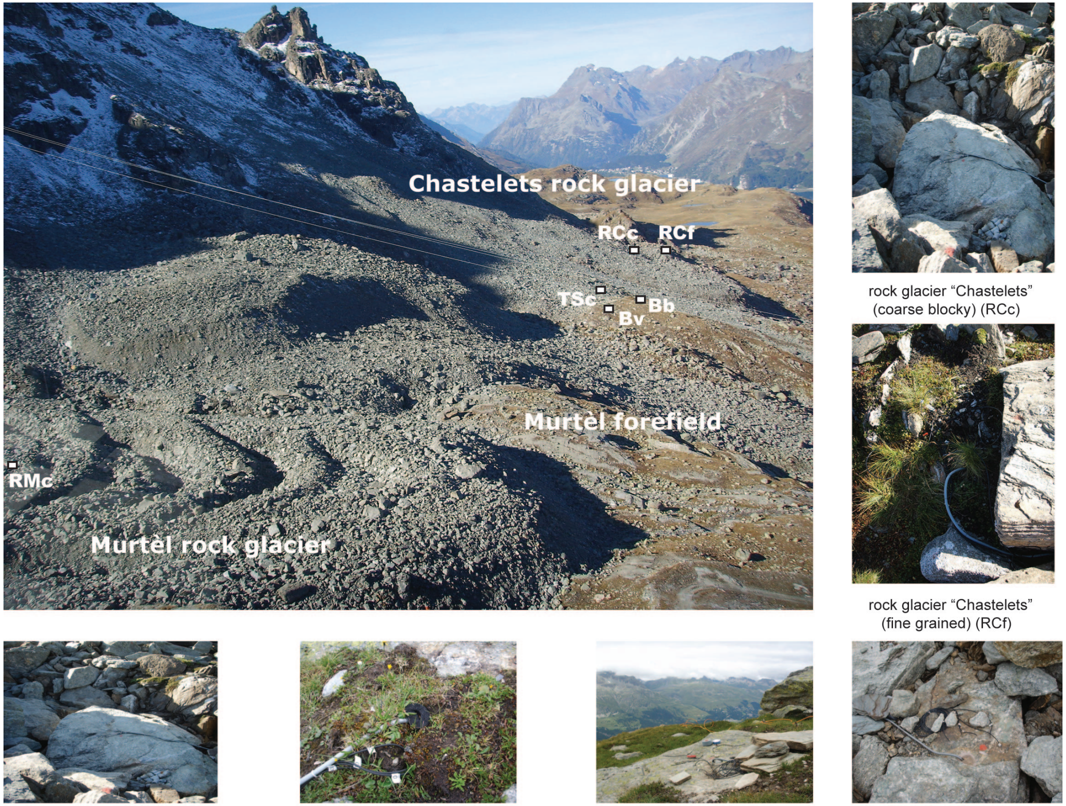

Fig. 2. Photographs of the different surfaces at the borehole locations in the investigation area, (August 2009).

TCD
5, 2629–2663, 2011

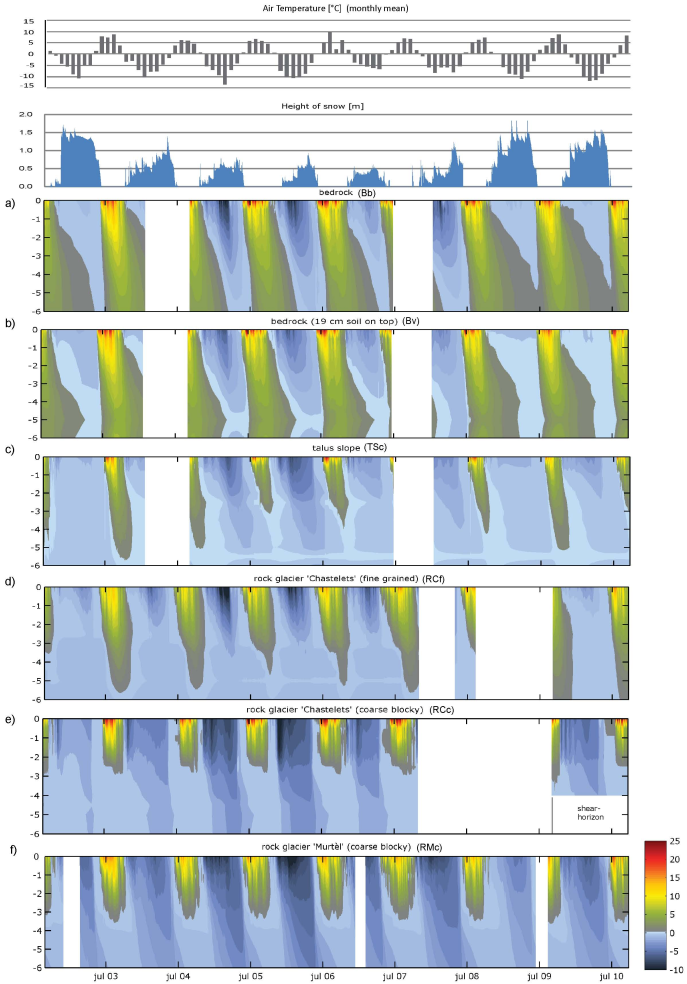

Fig. 3. Borehole temperature data from 2002–2010.

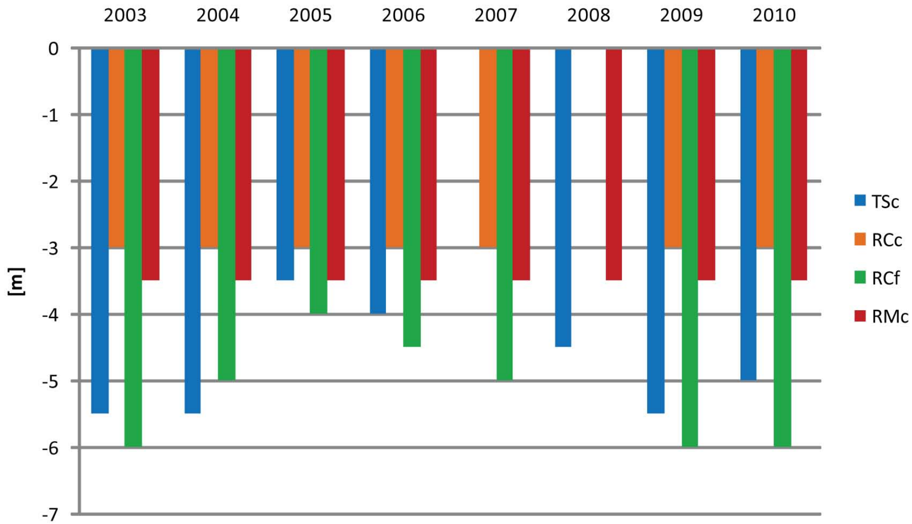

Fig. 4. Active layer depth of the last eight years for the boreholes with permafrost.

TCD
5, 2629–2663, 2011

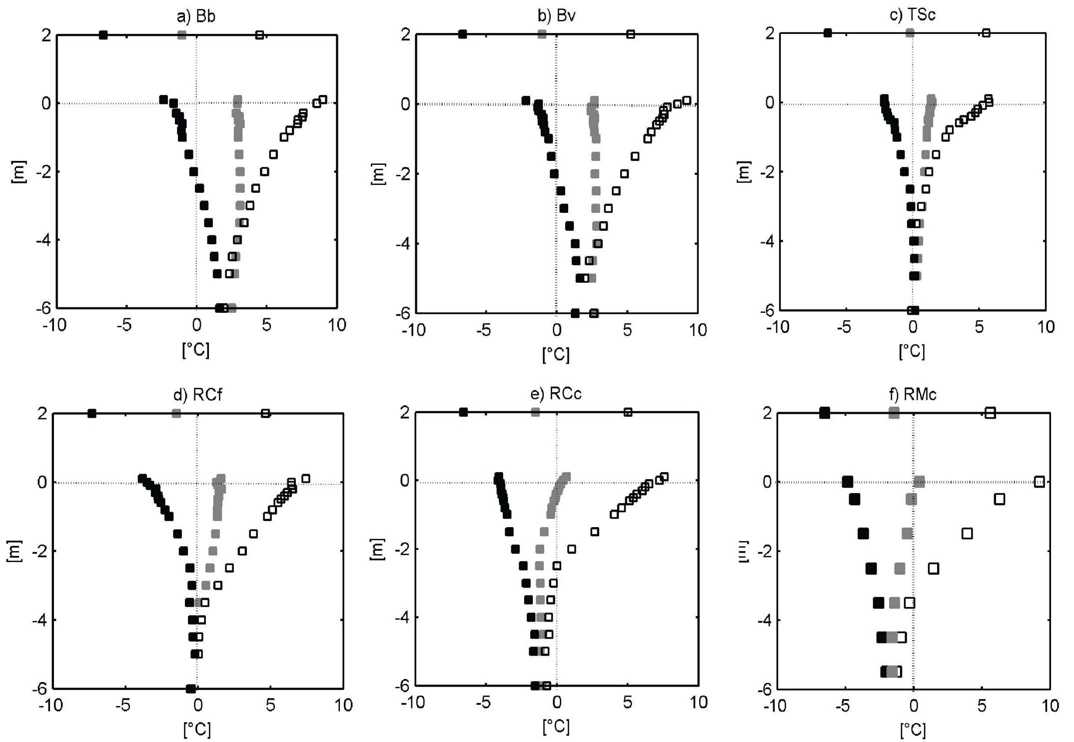

Fig. 5. Eight year mean annual (grey), mean summer (white) and mean winter temperatures (black) for each borehole and each depth. In addition, air temperature (taken from the micrometeorological station at rock glacier Murtel) and the individual mean GST at each borehole site are included.

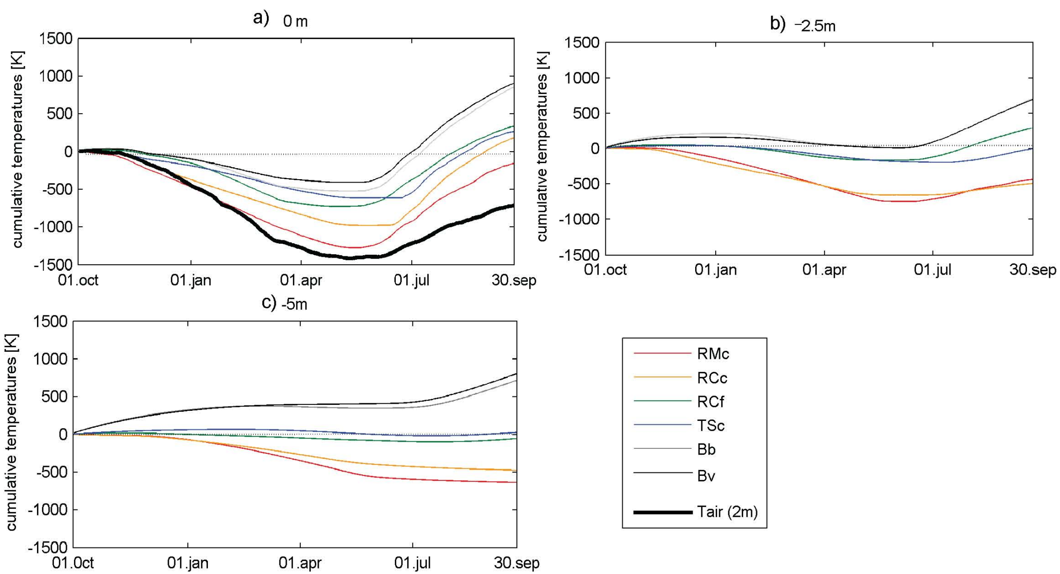

Fig. 6. Mean cumulative temperatures (averaged over four years – 2003, 2005, 2006, 2010) at three different depths – 0 m **(a)**, 2.5 m **(b)** and 5 m **(c)** – for the six boreholes. The air temperature is shown for comparison.

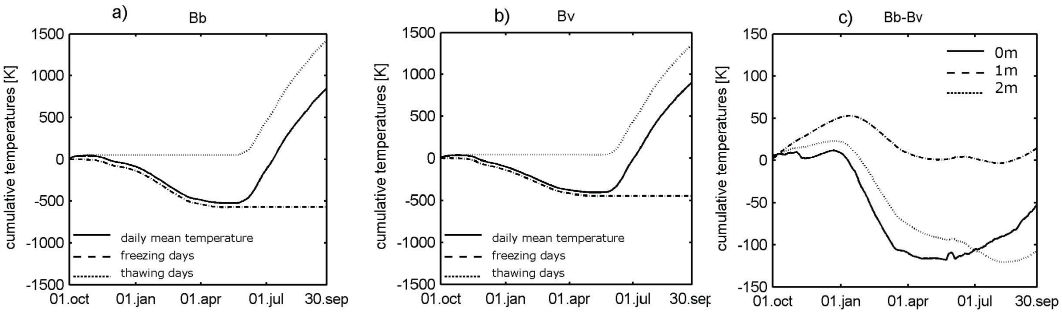

Fig. 7. Cumulative temperatures (averaged over four years – 2003, 2005, 2006, 2010) at the surface (0 m depth) for bare bedrock (Bb) and vegetated bedrock (Bv). Freezing degree days are all days ≤0 °C, whereas the days with temperatures >0 °C were set to 0. Likewise the thawing degree days are the days with temperatures > 0 °C and temperatures ≤0 °C were set to 0. For **(c)** the mean cumulated temperature difference between the vegetated and the bare bedrock site for 0 m, 1 m and 2 m depth was calculated.

TCD
5, 2629–2663, 2011

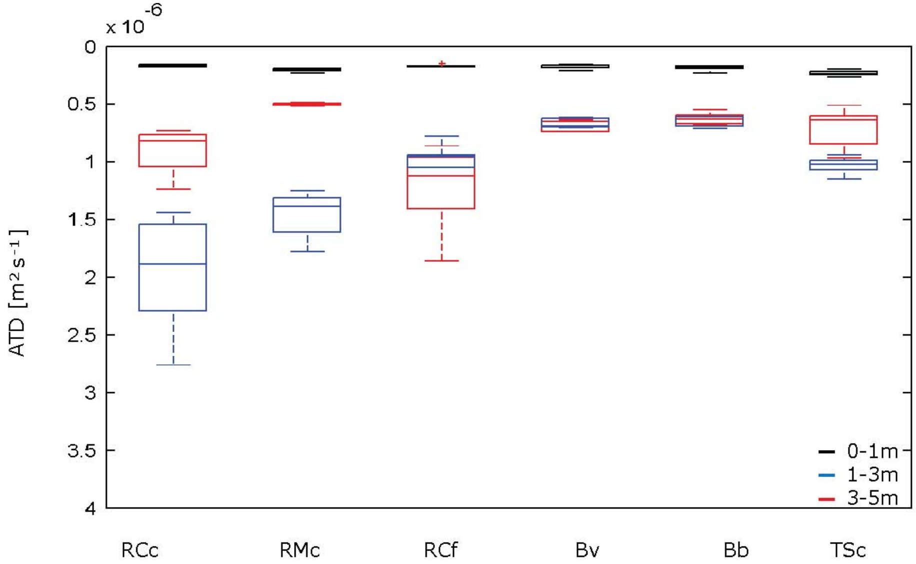

Fig. 8. ATD of the different sites, calculated as 6 year mean.

TCD
5, 2629–2663, 2011

Influence of surface heterogeneity on observed borehole temperatures

S. Schneider et al.

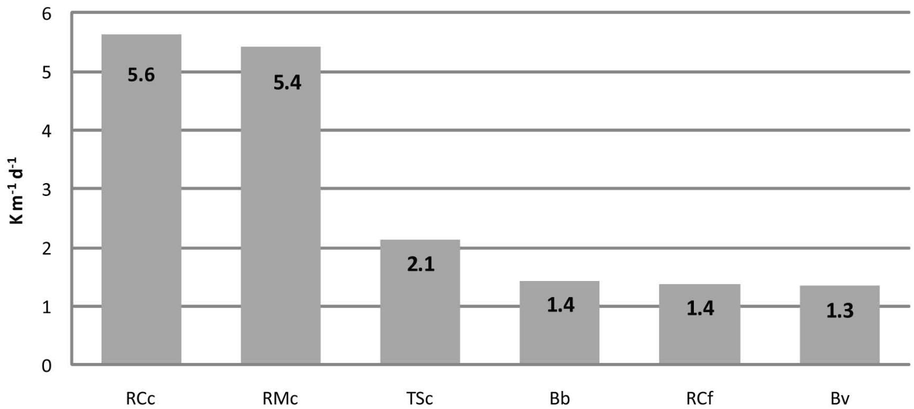

Fig. 9. Temperature transfer rate, calculated as 6 year mean from maximum summer borehole temperatures from 0.5 m depth to TTOP in $K\,m^{-1}\,d^{-1}$.

TCD
5, 2629–2663, 2011